



# Holographic Lifshitz superconductors with Weyl correction

Jun-Wang Lu<sup>1,2,a</sup>, Ya-Bo Wu<sup>3,b</sup>, Bao-Ping Dong<sup>1</sup>, Yu Zhang<sup>4</sup>

<sup>1</sup> School of Physics and Electronics, Qiannan Normal University for Nationalities, Duyun 558000, People's Republic of China

<sup>2</sup> CAS Key Laboratory of Theoretical Physics, Institute of Theoretical Physics, Chinese Academy of Sciences, Beijing 100190, People's Republic of China

<sup>3</sup> Department of Physics, Liaoning Normal University, Dalian 116029, People's Republic of China

<sup>4</sup> Faculty of Science, Kunming University of Science and Technology, Kunming 650500, People's Republic of China

Received: 6 February 2020 / Accepted: 9 November 2020 / Published online: 18 November 2020

© The Author(s) 2020

**Abstract** At the probe approximation, we construct a holographic  $p$ -wave conductor/superconductor model in the five-dimensional Lifshitz black hole with the Weyl correction via both numerical and analytical methods, and study the effects of the Lifshitz parameter  $z$  as well as the Weyl parameter  $\gamma$  on the superconductor model. As we take into account one of the two corrections separately, the increasing  $z$  ( $\gamma$ ) inhibits (enhances) the superconductor phase transition. When the two corrections are considered comprehensively, they display the obviously competitive effects on both the critical temperature and the vector condensate. In particular, the promoting effects of the Weyl parameter  $\gamma$  on the critical temperature are obviously suppressed by the increasing Lifshitz parameter. Meanwhile, in the case of  $z < 2.35$  ( $z > 2.35$ ), the condensate at lower temperature decreases (increases) with the increasing Weyl parameter  $\gamma$ . What is more, the difference among the condensate with the fixed Weyl parameter ( $\gamma = -\frac{6}{100}, 0, \frac{4}{100}$ ) decreases (increases) with the increasing Lifshitz parameter  $z$  in the region  $z < 2.35$  ( $z > 2.35$ ). Furthermore, the increasing  $z$  obviously suppresses the real part of conductivity for all value of the Weyl parameter  $\gamma$ . In addition, the analytical results agree well with the ones from the numerical method.

## 1 Introduction

The AdS/CFT correspondence which maps a gravity in a  $(d + 1)$ -dimensional AdS spacetime to a conformal field theory on the  $d$ -dimensional boundary opens up a new window to investigate the strongly coupled gauge field theory [1, 2]. In the recent years, the AdS/CFT correspondence (and its generalized version, gauge/gravity duality) has been applied

extensively to study many strong correlated systems [3–6], especially the high temperature superconductor [7, 8].

In 2008, the authors in Ref. [7] constructed numerically a holographic  $s$ -wave conductor/superconductor model in the Einstein–Abelian–Higgs system within the probe limit. The model displays that the scalar field begins to condense as the temperature drops below the critical point, which is accompanied by spontaneous breaking of the  $U(1)$  symmetry. Meanwhile, the infinite DC conductivity can be observed by studying the fluctuations of the vector potential  $A_x$  in the bulk [7], following which the authors in Ref. [9] modeled the Meissner effect and argued that the holographic superconductor behaves as a type II superconductor. Subsequently, Ref. [10] constructed the vortex lattice solution in a  $(2+1)$ -dimensional holographic superconductor model. What is more, Refs. [11, 12] studied the holographic superconductor by the analytical Sturm–Liouville (S–L) eigenvalue method and obtained the critical temperature as well as the critical exponent of the condensate which uphold the numerical results.

Due to the fact that series of main properties of superconductors have been realized successfully by the gauge/gravity duality, holographic superconductors became the most interesting topic and were studied widely from various aspects in the past decade. One of the main developing direction is naturally to construct the superconductor model much closer to the real superconductor in the condensed physics. For example, superconductor models were extended to the  $SU(2)$  Yang–Mills  $p$ -wave model [13], the  $d$ -wave model [14, 15], the superfluid model [16, 17], the coexistence and competition of multiple orders as well as the intertwined order [5, 18–23], the lattice [24–26] and their corresponding insulator/superconductor phase transition model [27]. In particular, considering that the phase transitions in many condensed matter systems exhibit the anisotropic scaling of spacetime, the authors in Refs. [28, 29] proposed a  $(d + 2)$ -

<sup>a</sup> e-mail: [lujunwang.2008@163.com](mailto:lujunwang.2008@163.com) (corresponding author)

<sup>b</sup> e-mail: [ybwu61@163.com](mailto:ybwu61@163.com)

dimensional non-relativistic gravity with the Lifshitz fixed point,  $t \rightarrow b^z t$ ,  $\vec{x} \rightarrow b\vec{x}$  ( $z \neq 1$ ) as

$$ds^2 = L^2 \left( -r^{2z} f(r) dt^2 + \frac{dr^2}{r^2 f(r)} + r^2 \sum_{i=1}^d dx_i^2 \right),$$

$$f(r) = 1 - \frac{r_+^{z+d}}{r^{z+d}}, \quad (1)$$

where  $r_+$  denotes the event horizon and the Hawking temperature reads  $T = \frac{(z+d)r_+^z}{4\pi}$  and also the dynamical critical exponent  $z$  represents the anisotropy of the spacetime. Obviously, the geometry (1) reduces to the AdS spacetime for  $z = 1$ , while it is a gravity dual with the Lifshitz scaling as  $z > 1$ .<sup>1</sup> Based on the Lifshitz background (1),  $s$ -wave and  $p$ -wave superconductor models were constructed [30–36]. It was shown that for both  $s$ -wave and  $p$ -wave superconductors, the increasing Lifshitz parameter inhibits the phase transition and suppresses the conductivity and also softens the energy gap. Meanwhile, imitating the holographic  $s$ -wave superconductor model, a magnetic-field-induced vector condensate was realized via a Maxwell-complex-vector (MCV) field with a mass [37], which was verified to be a generalization of the  $SU(2)$   $p$ -wave model with a mass [38–40]. The MCV model was then used to construct the electric-field-induced superconductor model [41–43]. By considering the backreaction from MCV field to the gravitational background, the model showed the abundant phase structure, such as “zero-order phase transition” and “the retrograde condensate” in the four-dimensional AdS black hole [21, 22, 44–46]. Furthermore, the stronger backreaction inhibits the superconductor phase transition in the three-dimensional BTZ (Bandos–Teitelboim–Zanelli) black hole [44]. What is more, we constructed the MCV  $p$ -wave superconductor model in the Lifshitz gravity, and found that the increasing Lifshitz parameter makes the vector condensate more difficult to form [47].

The other developing direction is to improve the basic framework of the gauge/gravity duality by investigating the influences of the  $1/\lambda$  ( $\lambda$  is the 't Hooft coupling) corrections on the holographic models. Concretely, the related works involve the high curvature corrections such as the Gauss–Bonnet gravity [20, 39, 48–51], Quasi-topological gravity [52], Horava–Lifshitz gravity [53] and nonlinear electrodynamics, for example, Born–Infeld correction [54], exponential correction [55], Logarithmic correction [56]. The above two kinds of corrections were found to inhibit the phase transition. The third kind of interesting correction composes of the curvature tensor and the gauge field strength, such as the  $RF^2$  correction, especially the Weyl correction made up

of the Weyl tensor and the Maxwell field strength, which was firstly introduced to realize the breakdown of the electromagnetic self-duality from a holographic perspective [57]. Concretely, the holographic  $s$ -wave and MCV  $p$ -wave superconductor models were constructed with the Weyl correction in Refs. [58–60]. It was followed that the Weyl correction does not influence the properties of the  $p$ -wave insulator/superconductor phase transition but enhances both  $s$ -wave and MCV  $p$ -wave conductor/superconductor phase transitions. Subsequently, a general high derivative theory was proposed in Ref. [61], which extends the works in Refs. [58–60]. By considering the six derivative term in Ref. [61], the authors in Refs. [62–64] constructed the  $s$ -wave and MCV  $p$ -wave conductor/superconductor phase transition models via the numerical and analytical methods, respectively, and found that the increasing six derivative correction enhances the superconductor phase transition.

Given by the opposite effects between the Lifshitz scaling and the Weyl correction, it is natural to ask whether we can see the interesting competition on the Lifshitz superconductor model with the Weyl correction. Meanwhile, in order to further understand the influences of the  $1/\lambda$  correction on the holographic model, in this work, we are going to study systematically the effects of the Lifshitz dynamical exponent  $z$  and the Weyl parameter  $\gamma$  on the holographic MCV  $p$ -wave superconductor in the five-dimensional Lifshitz black hole with Weyl correction. The results show that both the Lifshitz parameter  $z$  and the Weyl parameter  $\gamma$  together control the critical temperature and the vector condensate as well as the frequency dependent conductivity.

This paper is planed as follows. In Sect. 2, we realize numerically the  $p$ -wave conductor/superconductor phase transition and then study the frequency dependent conductivity, following which the superconductor model is reconstructed by the analytical method. The final section is devoted to the conclusions and discussions. In the appendix, we list the concrete coefficients ( $\mathcal{C}_i$ ) about the equations in Sect. 2.

## 2 Holographic superconductor model

In this section, we firstly construct the holographic  $p$ -wave superconductor model in the five-dimensional Lifshitz black hole with Weyl correction via the numerical method. To verify that below the critical temperature the hairy state is indeed stable, we compare the grand potential of the hairy state with the no hairy state. So as to investigate the influences of the Lifshitz parameter as well as the Weyl correction, we also study the frequency dependent conductivity, following which we restudy the superconductor model by the analytical S-L method to testify the numerical results.

To introduce the massive MCV field in the five-dimensional Lifshitz black hole with Weyl correction [28, 29, 37, 45, 46,

<sup>1</sup> It should be noted that at present we only focus on the discussion of the Lifshitz black hole, but not take into account the following curvature correction (i.e., the Weyl term) from the matter field part.

61,63], we take the full action as

$$\begin{aligned}
 S &= \frac{1}{16\pi G_{d+2}} \int d^{d+2}x \sqrt{-g} (\mathcal{L}_g + \mathcal{L}_m), \\
 \mathcal{L}_g &= R - 2\Lambda - \frac{1}{2} \partial_\mu \varphi \partial^\mu \varphi - \frac{1}{4} e^{\iota\varphi} \mathcal{F}_{\mu\nu} \mathcal{F}^{\mu\nu}, \\
 \mathcal{L}_m &= -\frac{1}{8} F_{\mu\nu} X^{\mu\nu\rho\sigma} F_{\rho\sigma} - \frac{1}{2} \rho_{\mu\nu}^\dagger \rho^{\mu\nu} \\
 &\quad - m^2 \rho_\mu^\dagger \rho^\mu + i q \gamma_0 \rho_\mu \rho_\nu^\dagger F^{\mu\nu}, \tag{2}
 \end{aligned}$$

where the gravitational part  $\mathcal{L}_g$  is made up of the Ricci scalar  $R$ , the cosmological constant  $\Lambda$ , the massless scalar field  $\varphi$  and an abelian gauge field characterized by  $\mathcal{F}^{\mu\nu}$  with the parameter  $\iota$  depending on the Lifshitz parameter  $z$  and the dimension of spacetime  $d$ . By considering only this part  $\mathcal{L}_g$ , one can obtain the  $(d + 2)$ -dimensional Lifshitz black hole solution (1). The second part  $\mathcal{L}_m$  is used to describe the vector condensate with the Weyl correction. Concretely, the matter part  $\mathcal{L}_m$  consists of a vector field  $\rho_\mu$  and a Maxwell field  $F_{\mu\nu}$  coupled to the Weyl tensor  $C_{\mu\nu}^{\rho\sigma}$ , where the antisymmetry tensor  $\rho_{\mu\nu} = D_\mu \rho_\nu - D_\nu \rho_\mu$  and  $D_\mu = \nabla_\mu - i q A_\mu$ ,  $F_{\mu\nu} = \nabla_\mu A_\nu - \nabla_\nu A_\mu$  and  $m$  ( $q$ ) is the mass (charge) of  $\rho_\mu$ . Meanwhile, the tensor  $X_{\mu\nu}^{\rho\sigma}$  is an infinite family of high derivative terms, i.e.,

$$\begin{aligned}
 X_{\mu\nu}^{\rho\sigma} &= I_{\mu\nu}^{\rho\sigma} - 8\gamma_{1,1} L^2 C_{\mu\nu}^{\rho\sigma} - 4L^2 \gamma_{2,1} C^2 I_{\mu\nu}^{\rho\sigma} \\
 &\quad - 8L^4 \gamma_{2,2} C_{\mu\nu}^{\alpha\beta} C_{\alpha\beta}^{\rho\sigma} \\
 &\quad - 4L^6 \gamma_{3,1} C^3 I_{\mu\nu}^{\rho\sigma} - 8L^6 \gamma_{3,2} C^2 I_{\mu\nu}^{\rho\sigma} \\
 &\quad - 8L^6 \gamma_{3,3} C_{\mu\nu}^{\alpha_1\beta_1} C_{\alpha_1\beta_1}^{\alpha_2\beta_2} C_{\alpha_2\beta_2}^{\rho\sigma} + \dots, \tag{3}
 \end{aligned}$$

where  $I_{\mu\nu}^{\rho\sigma} = \delta_\mu^\rho \delta_\nu^\sigma - \delta_\mu^\sigma \delta_\nu^\rho$  is an identity matrix and  $C^n = C_{\mu\nu}^{\alpha_1\beta_1} C_{\alpha_1\beta_1}^{\alpha_2\beta_2} \dots C_{\alpha_{n-1}\beta_{n-1}}^{\mu\nu}$ . In the remainder of this paper, we focus on the Weyl correction and thus only turn on the first two terms in Eq. (3), i.e.,

$$\begin{aligned}
 &-\frac{1}{8} F^{\mu\nu} \left( I_{\mu\nu}^{\rho\sigma} - 8\gamma_{1,1} L^2 C_{\mu\nu}^{\rho\sigma} \right) F_{\rho\sigma} \\
 &= -\frac{1}{4} F_{\mu\nu} F^{\mu\nu} + \gamma_{1,1} L^2 F^{\mu\nu} C_{\mu\nu}^{\rho\sigma} F_{\rho\sigma} \tag{4}
 \end{aligned}$$

with other  $\gamma_{i,j}$  terms in Eq. (3) vanishing, which clearly restores to the case in Refs. [58–60]. For simplicity, we will take  $L = 1$  and rename  $\gamma_{1,1} = \gamma$  throughout the paper and further restrict the range of the Weyl parameter as  $\gamma \in [-\frac{6}{100}, \frac{4}{100}]$  following Refs. [57–59]. In addition, by rescaling  $A_\mu \rightarrow \tilde{A}_\mu/q$  and  $\rho_\mu \rightarrow \tilde{\rho}_\mu/q$ , a factor  $1/q^2$  will appear in front of the matter part  $\mathcal{L}_m$ . Naturally, by taking the limit  $q \rightarrow \infty$  with  $\tilde{A}_\mu$  and  $\tilde{\rho}_\mu$  fixed, the backreaction of the matter fields on the Lifshitz geometry (1) will be suppressed so that we can work in the so-called probe limit. Thus, varying the action (2) with respect to the vector field  $\rho_\mu$  and the gauge field  $A_\mu$ , respectively, we read off the equations of

motion

$$D_\mu \rho^{\mu\nu} - m^2 \rho^\nu + i \gamma_0 \rho_\mu F^{\mu\nu} = 0, \tag{5}$$

$$\begin{aligned}
 &\frac{1}{2} \nabla_\mu (X^{\mu\nu\rho\sigma} F_{\rho\sigma}) - i \gamma_0 \nabla_\mu (\rho^\mu (\rho^\nu)^\dagger - \rho^\nu (\rho^\mu)^\dagger) \\
 &\quad + i ((\rho_\mu)^\dagger \rho^{\mu\nu} - \rho_\mu (\rho^{\mu\nu})^\dagger) = 0. \tag{6}
 \end{aligned}$$

To build the  $p$ -wave superconductor induced by the electric field, the ansatzs for the vector field  $\rho_\mu$  and the gauge field  $A_\mu$  can be taken as the following form [37,45,46],

$$\rho_\nu dx^\nu = \psi_x(r) dx, \quad A_\nu dx^\nu = \phi(r) dt, \tag{7}$$

with other components vanishing.

Thus Eqs. (5) and (6) in the background (1) with  $d = 3$  reduce to

$$\begin{aligned}
 &\psi_x''(r) + \left( \frac{z+2}{r} + \frac{f'(r)}{f(r)} \right) \psi_x'(r) \\
 &\quad + \left( \frac{\phi^2(r)}{r^{2z+2} f^2(r)} - \frac{m^2}{r^2 f(r)} \right) \psi_x(r) = 0, \tag{8}
 \end{aligned}$$

$$\mathcal{C}_1 \phi''(r) + \mathcal{C}_2 \phi'(r) - \frac{2\psi_x^2(r)}{r^4 f(r)} \phi(r) = 0, \tag{9}$$

where the prime stands for the derivative with respect to  $r$ . In particular, as  $z = 1$  Eqs. (8) and (9) restore to the pure Weyl case in Ref. [59], and if one requires further  $\gamma = 0$ , the current model returns back to the  $p$ -wave superconductor model in the standard AdS black hole [46].

To solve the above coupled differential equations, we usually impose the boundary conditions. At the horizon  $r = r_+$ , we require  $\phi(r_+) = 0$  to satisfy the finite norm of  $A_\mu$ , while  $\psi_x(r_+)$  needs to be regular. At the infinite boundary ( $r \rightarrow \infty$ ),  $\psi_x(r)$  and  $\phi(r)$  behave as

$$\psi_x(r) = \frac{\psi_1}{r^{\Delta_-}} + \frac{\psi_2}{r^{\Delta_+}} + \dots, \tag{10}$$

$$\phi(r) = \mu - \frac{\rho}{r^{3-z}} + \dots (z < 3), \tag{11}$$

where  $\Delta_\pm = \frac{z+1 \pm \sqrt{(z+1)^2 + 4m^2}}{2}$ . It is worth noting that the asymptotical solution for  $\phi(r)$  behaves as  $\mu - \rho \ln r + \dots$  in the case of  $z = 3$  and  $\mu - \rho r^{z-3} + \dots$  for  $z > 3$ , which is obviously divergent at infinity. Similar divergent phenomenon also exists in the four-dimensional Lifshitz black hole with  $z \geq 2$ . Although there are some works investigating the Lifshitz effects on the critical behavior with  $z \geq 3$  ( $z \geq 2$ ) in the five (four)-dimensional Lifshitz black hole [65,66], we still wish that the gauge field decays at infinity and has the falling off form. Therefore, we focus on the superconductor model with the Lifshitz parameter space  $z < 3$  in the present paper. Meanwhile, the constants  $\psi_1$  ( $\psi_2$ ),  $\mu$  ( $\rho$ ) are interpreted as the source (the vacuum expectation value) of the dual operator  $\hat{J}_x$  and the chemical potential (the charge density) of dual field theory, respectively. By requiring that the U(1) symmetry is broken spontaneously, we impose the source-free condition

$\psi_1 = 0$ . We take  $\Delta = \Delta_+ = 2$  throughout the paper, which implies that the mass squared of the vector field  $m^2 = 2 - 2z$ . For the above coupled equations and the asymptotical behaviors of  $\psi_x$  and  $\phi$ , there exists an important scaling symmetry, such as  $r \rightarrow \xi r$ ,  $(T, \mu) \rightarrow \xi^z (T, \mu)$ ,  $(\psi_2, \rho) \rightarrow \xi^3 (\psi_2, \rho)$  with  $\xi$  a constant, by using which we can fix the chemical potential  $\mu$  and thus work in the grand canonical ensemble.

## 2.1 Numerical part

In the current paper, we will do the numerical calculations on the Mathematica software by means of the shooting method. In particular, we numerically solve Eqs. (8) and (9) with the given boundary conditions by modifying and improving the numerics developed by the authors in Ref. [7]. During the calculation, we set the Working precision of the Mathematica program to be 30 but only record four significant digits of numerical results in the work, which guarantees our results to be reliable. Meanwhile, as mentioned above, the Lifshitz scaling and the Weyl correction are introduced in the superconductor model from the different points of view, therefore, we can study the effects of the Lifshitz parameter  $z$  and the Weyl parameter  $\gamma$  on the superconductor model separately.

After numerical calculations, we obtain the vector condensate as a function of the temperature for various Lifshitz parameter  $z$  and Weyl parameter  $\gamma$ . To see clearly the effect of the Weyl correction parameter  $\gamma$  on the vector condensate, we typically display the condensate for  $\gamma = -\frac{6}{100}, 0, \frac{4}{100}$  with the fixed Lifshitz parameter  $z = 1$  (left panel) and  $\frac{5}{2}$  (right panel) in Fig. 1. It is observed that there always exists a critical temperature below which the vector hair starts to condense. From the analysis and fitting of the condensate curve near the critical point, we find all curves of condensate versus the temperature have a square root behavior near the critical value, which indicates that the system might suffer from a second-order phase transition at the critical temperature. Meanwhile, at the lower temperature, the vector condensate approximates a stable value in the case of  $z = 1$ , which decreases with the increasing Weyl correction parameter  $\gamma$ . However, at the lower temperature, the condensate for  $z > 1$  shows an obvious increasing trend rather than a steady value with the decreasing temperature, for example, the case of  $z = \frac{5}{2}$  in the right panel of Fig. 1, which is quite different from the case of  $z = 1$  and might be the universal characters for the Lifshitz superconductor [34]. The most interesting thing is that the condensate decreases with the increasing Weyl parameter for small enough Lifshitz parameter and increases with the increasing Weyl parameter for large enough Lifshitz parameter (for example the case in the right panel of Fig. 1 with  $z = \frac{5}{2}$ ). By careful calculation, the point of demarcation of the Lifshitz parameter is about  $z_d \approx 2.35$ , where the condensate is almost independent of the Weyl parameter  $\gamma$ .

In other words, the difference among the condensate curves for the fixed Weyl parameter ( $\gamma = -\frac{6}{100}, 0, \frac{4}{100}$ ) decreases with the increasing Lifshitz parameter  $z$  when  $z < z_d$  and vanishes at  $z = z_d$  and then increases with the increasing Lifshitz parameter when  $z > z_d$ . Furthermore, we also consider the case for other value of  $\gamma$  and  $z$ , the results show that the effects of the Weyl parameter on the condensate in the presence of Lifshitz correction is qualitative the same. Especially, in the case of  $z = 1$ , the result restores to the pure Weyl superconductor [59].

In order to disclose sufficiently the interaction between the Weyl correction and the Lifshitz correction, we also display the condensate for  $z = 1, \frac{3}{2}, \frac{5}{2}$  with the fixed Weyl correction parameter  $\gamma = -\frac{6}{100}$  (left panel) and  $\frac{4}{100}$  (right panel) in Fig. 2. It is obviously observed that at the lower temperature the condensate for  $z > 1$  does not become stable like the  $z = 1$  case but still increases with the decreasing temperature, especially for the case of  $\gamma = \frac{4}{100}$  in the right panel of the figure. Furthermore, the condensate grows faster with the increasing Lifshitz parameter  $z$  at the lower temperature. However, the vector condensate grows more slowly with the increasing Lifshitz parameter  $z$  near the critical temperature. Comprehensively speaking, it is quite reasonable that the condensate curves intersect with each other for different Lifshitz parameter. In particular, we take the value of  $\frac{T}{T_c}$  as the horizontal coordinate, which suggests that we have moved the starting location of the condensate to the same point in the figure.

To obtain synthetically the Lifshitz and Weyl effects on the critical temperature, we show the critical temperature versus the Weyl parameter  $\gamma$  for different Lifshitz parameter  $z$  in the left panel of Fig. 3 and list the related results in Table 1, from which we can see that both the Weyl correction and the Lifshitz parameter affect obviously the critical temperature. In particular, for all values of the Lifshitz parameter  $z$ , the critical temperature increases with the larger Weyl correction parameter  $\gamma$ , which means that the larger Weyl correction enhances the conductor/superconductor phase transition. While for the fixed Weyl correction, the critical temperature decreases with the Lifshitz parameter  $z$ , which means that the stronger anisotropy of the spacetime makes the conductor/superconductor phase transition more difficult. Comprehensively speaking, the curve of the critical temperature versus the Weyl correction becomes flatter with the increasing Lifshitz parameter  $z$ , which means that the promoting effect of Weyl correction on the phase transition is suppressed by the increasing Lifshitz correction. We attribute this phenomenon to the competition between the Lifshitz scaling and the Weyl correction. Additionally, after rescaling the vector field and the gauge field by the charge density, we can switch the superconductor model from the grand canonical ensemble to the canonical ensemble. Especially, the values

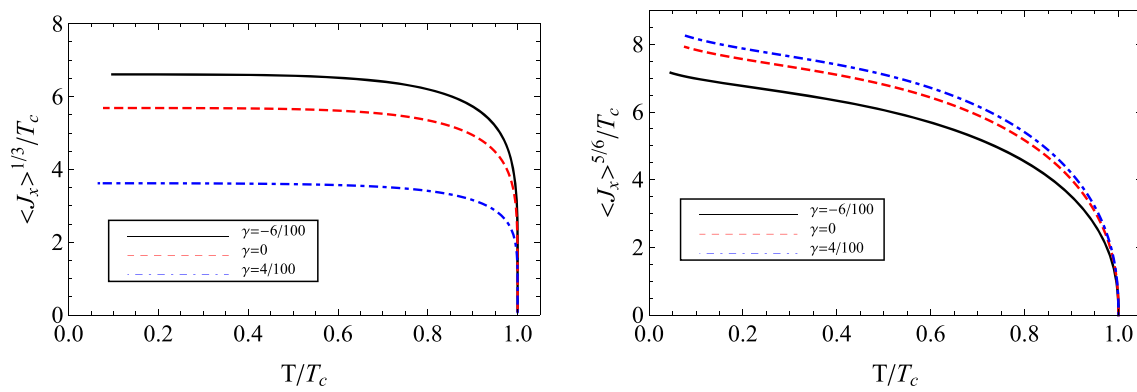


**Fig. 1** The condensate versus the temperature with  $\gamma = -\frac{6}{100}$  (black solid),  $\gamma = 0$  (red dashed),  $\gamma = \frac{4}{100}$  (blue dotdashed) for the fixed value  $z = 1$  (the left panel) and  $z = \frac{5}{2}$  (the right panel)

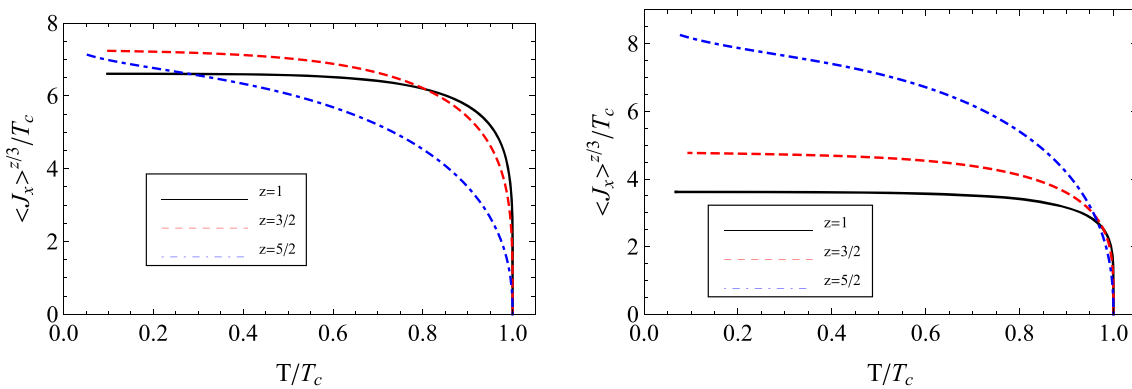


**Fig. 2** The condensate versus the temperature with  $z = 1$  (black solid),  $z = \frac{3}{2}$  (red dashed),  $z = \frac{5}{2}$  (blue dotdashed) for the fixed value  $\gamma = -\frac{6}{100}$  (the left panel) and  $\gamma = \frac{4}{100}$  (the right panel)

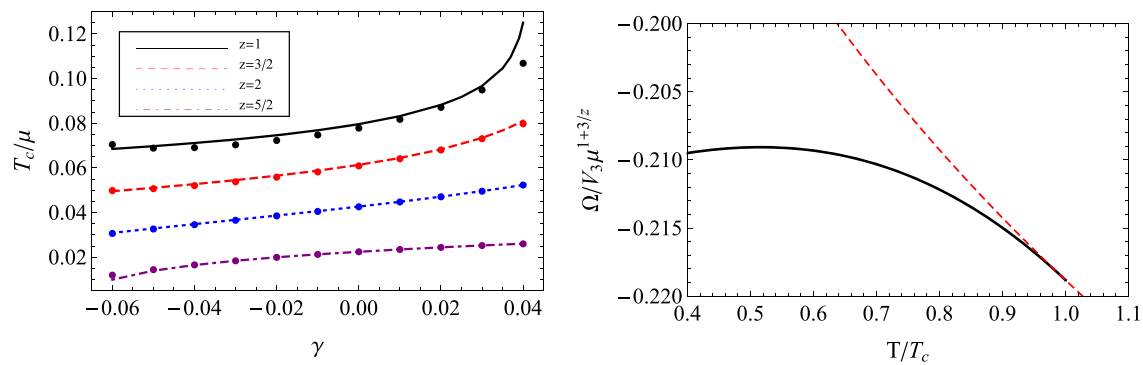


**Fig. 3** The critical temperature versus the Weyl parameter  $\gamma$  for  $z = 1$  (black solid),  $z = \frac{3}{2}$  (red dashed),  $z = 2$  (blue dotdashed),  $z = \frac{5}{2}$  (purple dotted) (left) and the grand potential about the normal state (red dashed) and the superconducting state (black solid) in the case of  $z = \frac{6}{5}$  and  $\gamma = -\frac{1}{20}$  (right)

of the critical temperature for  $z = 1$  and  $\gamma = -0.02, 0, 0.02$  listed in Table 1 are rewritten as  $\frac{T_c}{\rho^{1/3}} = 0.18767(\gamma = -0.02), 0.20052(\gamma = 0), 0.22244(\gamma = 0.02)$ , which obviously return to the Weyl superconductor in Ref. [59].

To check that below the critical point the superconducting state is indeed thermodynamically favored compared with the normal state, it is helpful to calculate the grand potential of

the system, which is defined by the Euclidean on-shell action  $S_E$  timing the temperature of the black hole, i.e.,  $\Omega = T S_E$ . Integrating the Minkowski action (2) by parts yields the on-shell part of action as

**Table 1** The critical temperature in unit of chemical potential  $\mu$  from the numerical method ( $T_{cn}$ ) and the analytical method ( $T_{ca}$ ) for different value of  $\gamma$  and  $z$

$\gamma$	-0.06	-0.04	-0.02	0	0.02	0.04
$T_{cn}(z = 1)$	0.06846	0.07111	0.07459	0.07958	0.08819	0.12503
$T_{ca}(z = 1)$	0.07045	0.06904	0.07225	0.07779	0.08706	0.10682
$T_{cn}(z = 3/2)$	0.04954	0.05271	0.05649	0.06133	0.06827	0.08114
$T_{ca}(z = 3/2)$	0.04982	0.05204	0.05583	0.06088	0.06801	0.07974
$T_{cn}(z = 2)$	0.03087	0.03480	0.03865	0.04266	0.04709	0.05236
$T_{ca}(z = 2)$	0.03063	0.03456	0.03848	0.04256	0.04703	0.05229
$T_{cn}(z = 5/2)$	0.00993	0.01648	0.01996	0.02240	0.02441	0.02603
$T_{ca}(z = 5/2)$	0.01196	0.01655	0.01992	0.02241	0.02437	0.02595

$$\begin{aligned}
 S_{os} &= \int \sqrt{-g} d^5x (2\gamma \nabla_\mu (A_\nu C^{\mu\nu\rho\sigma} F_{\rho\sigma}) \\
 &\quad - \frac{1}{2} \nabla_\mu (A_\nu F^{\mu\nu}) - \nabla_\mu (\rho_\nu^\dagger \rho^{\mu\nu}) \\
 &\quad - \frac{i}{2} A_\nu (\rho_\mu^\dagger \rho^{\mu\nu} - \rho_\mu (\rho^{\mu\nu})^\dagger)) \\
 &= \frac{V_3}{T} \sqrt{\hbar} \left( 2\gamma n_r A_\nu C^{\nu\rho\sigma} F_{\rho\sigma} - \frac{1}{2} n_r A_\nu F^{r\nu} - n_r \rho_\nu^\dagger \rho^{r\nu} \right) \Big|_{r \rightarrow \infty} \\
 &\quad - \frac{V_3}{T} \frac{i}{2} \int \sqrt{-g} A_\nu (\rho_\mu^\dagger \rho^{\mu\nu} - \rho_\mu (\rho^{\mu\nu})^\dagger) dr,
 \end{aligned}$$

where we have taken into account  $\int d^3x = V_3, \int dt = \frac{1}{T}$  and also Eqs. (5) and (6). Reminding that  $S_E = -S_{os}$ , we obtain the density of the grand potential as

$$\begin{aligned}
 \frac{\Omega}{V_3} &= \frac{-TS_{os}}{V_3} = \frac{1}{2}(z-3)(1-4\gamma z+4\gamma z^2)\mu\rho \\
 &\quad + \int_{r_+}^\infty \frac{\phi^2 \psi^2}{r^z f} dr. \tag{12}
 \end{aligned}$$

Intuitively, both the Lifshitz parameter  $z$  and the Weyl parameter  $\gamma$  will affect the grand potential. Especially, in the case of  $z = 1$  and  $\gamma = 0$ , Eq. (12) returns to the pure Weyl correction [59] and the Lifshitz case [47], respectively. Next, we typically display the grand potential as a function of the temperature for the case of  $z = \frac{6}{5}, \gamma = -\frac{1}{20}$  in the right panel of Fig. 3. Near the critical temperature, the black solid curve corresponding to the superconducting state stretches out from the red dashed curve corresponding to the normal state smoothly with the decreasing temperature, which means that at the critical temperature the system indeed suffers from a second-order phase transition, and thus agrees with the behavior of the condensate in Figs. 1 and 2. Most importantly, the value of the grand potential of the superconducting state is always lower than that of the normal state, which means that below the critical temperature, the superconducting state is indeed thermodynamically stable. In addition, we also consider the other parameter cases, such as  $(z = \frac{5}{2}, \gamma = -\frac{6}{100}), (z = \frac{5}{2}, \gamma = \frac{4}{100}), (z = 1, \gamma = -\frac{6}{100})$  and  $(z = 1, \gamma = \frac{4}{100})$  as well as the case  $(z = \frac{3}{2}, \gamma = 0)$  and obtain the similar results to the case of  $(z = \frac{6}{5}, \gamma = -\frac{1}{20})$ .

As a result, it is believed our numerical results are reliable in the parameter space  $(1 \leq z \leq \frac{5}{2}, -\frac{6}{100} \leq \gamma \leq \frac{4}{100})$ .

As we all know, the infinite DC conductivity is one typical characteristic of superconductors. Meanwhile, the energy gap of the electric conductivity can help us to estimate how strong the interaction involves in the superconductor. As a result, it is useful to compute the AC conductivity of the superconductor model. From the AdS/CFT correspondence, to calculate the conductivity in the boundary field theory, we study the perturbation of the gauge field in the bulk. For simplicity, we turn on the perturbation along the  $y$  direction with the ansatz  $\delta A_y(t, r)dy = A_y(r)e^{-i\omega t}dy$ . Considering the matter field  $\psi_x(r)$  and the time component of gauge field  $\phi(r)$  in Eq. (7) and substituting the perturbed gauge field ansatz  $\delta A_y(t, r)dy$  into Eq. (6), we can derive the linearized equation of  $A_y(r)$  in the superconducting background, which is

$$\mathcal{C}_3 A_y''(r) + \mathcal{C}_4 A_y'(r) + \mathcal{C}_5 A_y(r) = 0. \tag{13}$$

At the horizon, we impose the ingoing wave condition

$$\begin{aligned}
 A_y(r) &= (r-r_+)^{-i\omega/(3+z)}(1 + A_{y1}(r-r_+) \\
 &\quad + A_{y2}(r-r_+)^2 + A_{y3}(r-r_+)^3 + \dots). \tag{14}
 \end{aligned}$$

While at the infinite boundary, the asymptotical solution of  $A_y(r)$  is of the form

$$A_y(r) = \begin{cases} A^{(0)} + \frac{A^{(2)}}{r^2} + \frac{A^{(0)}\omega^2}{2r^2} \ln \eta r + \dots, & z = 1, \\ A^{(0)} + \frac{A^{(z+1)}}{r} + \dots, & 1 < z < 3, \end{cases} \tag{15}$$

where  $A^{(i)}$ , and  $\eta$  are all constants. Combining with Eqs. (2) and (15), we can obtain the retarded Green's function as

$$G(\omega) = \begin{cases} 2\frac{A^{(2)}}{A^{(0)}} - \frac{1}{2}\omega^2, & z = 1, \\ \frac{(z+1)(3+4\gamma z-4\gamma z^2)}{3} \frac{A^{(z+1)}}{A^{(0)}}, & 1 < z < 3. \end{cases} \tag{16}$$

According to the Kubo formula, the AC conductivity reads

$$\sigma(\omega) = -\frac{i}{\omega} G(\omega). \tag{17}$$

To study the Weyl effect on the conductivity, we plot the AC conductivity at  $\frac{T}{T_c} \approx \frac{1}{2}$  for  $z = \frac{3}{2}$  with  $\gamma = -\frac{6}{100}$  (black),  $\gamma = 0$  (red),  $\gamma = \frac{4}{100}$  (blue) in the left panel of Fig. 4. It is observed from the imaginal part of conductivity at the lower frequency there is an obvious pole for all values of the Weyl parameter  $\gamma$ , which corresponds to a delta function of the DC conductivity as expected from condensed physics. Different from the  $z = 1$  case displayed in the right panel of Fig. 4, there does not exist the minimum for the imaginal part of the conductivity with  $z = \frac{3}{2}$  at the intermediate frequency in the left panel of Fig. 4. In fact, this result can be analyzed from the formula of the conductivity. According to Eq. (16), a frequency squared term appears for the  $z = 1$  case, which leads to the increasing behavior for the large enough frequency and thus produces a minimum at the intermediate frequency. However, as for the  $z > 1$  case, the frequency squared term vanishes, which results in the monotonically decreasing behavior for the imaginal part of conductivity. Correspondingly, the real part of conductivity becomes very soft. Nevertheless, if we define the location where the real part of conductivity grows the most rapidly as the energy gap, we can observe from the left panel of Fig. 4 that the energy gap decreases with the increasing Weyl correction parameter and is always larger than the value in the BCS superconductor, which is consistent with the effect of the Weyl correction on the condensate in Fig. 1. Meanwhile, in the large frequency region, the real part of conductivity increases monotonically, which seems to be the universal behavior for the holographic superconductor model in the five-dimensional gravitational spacetime [34,36,51]. In addition, we also calculate the conductivity for other values of the Lifshitz parameter, for example,  $z = \frac{5}{2}$ . The results show that the energy gap becomes much softer than the case with  $z = \frac{3}{2}$ .

In order to study the effect of the Lifshitz effects on the conductivity, we also calculate the AC conductivity for various value of  $z$  with fixed Weyl parameter  $\gamma$ . Typically, we plot frequency dependent conductivity at  $\frac{T}{T_c} \approx \frac{1}{2}$  for  $\gamma = -\frac{6}{100}$  with  $z = 1, \frac{3}{2}, \frac{5}{2}$  in the right panel of Fig. 4. It follows that the behaviors of the conductivity are similar to the case with fixed Lifshitz parameter (the left panel in Fig. 4) in the region for both low and high frequency. What is more, at the intermediate frequency region, there is not the minimum for the imaginal part of conductivity corresponding to the energy gap except the  $z = 1$  case. Furthermore, the real part of conductivity in the intermediate frequency is suppressed with the increasing Lifshitz parameter  $z$ , which is the typical effect of the Lifshitz correction on the conductivity and similar to the one on the conductivity for the  $s$ -wave case [34].

### 2.2 Analytical part

To check further the reliability of the numerical results in the previous subsection, especially the critical temperature, in what follows, we resolve the coupled equations (8) and (9) via the S-L eigenvalue method [11,59,62]. It should be mentioned that almost all the previous literature in terms of the analytical S-L superconductor model worked in the canonical ensemble [11,59,62], where the charge density is fixed. However, as for the present work calculated in the grand canonical ensemble with the fixed chemical potential, we should redefine the boundary condition of Eq. (9).

Introducing a new variable  $u = \frac{r_{\pm}}{r}$ , Eqs. (8) and (9) can be expressed as

$$\begin{aligned} \psi_x''(u) - \frac{3u^{z+3} + z}{u - u^{z+4}} \psi_x'(u) + \frac{m^2(u^{z+3} - 1) + u^{2z}\phi(u)^2}{u^2(u^{z+3} - 1)^2} \psi_x(u) &= 0, \\ \phi''(u) + C_6\phi'(u) + \frac{2\psi(u)^2}{(u^{z+3} - 1)(6\gamma(z - 5)u^{z+3} + 4\gamma(z - 1)z + 1)} \phi(u) &= 0, \end{aligned} \tag{18}$$

where the prime denotes the derivative with respect to  $u$ . As  $T = T_c$ , the condensate vanishes, i.e.,  $\psi(u) = 0$ , so we can rewrite Eq. (19) as

$$\phi''(u) + C_6\phi'(u) = 0. \tag{20}$$

Due to the existence of the Weyl correction parameter  $\gamma$ , in general, it is difficult to give the exact solution to Eq. (20). However, by regarding the Weyl parameter  $\gamma$  as a small quantity, we can solve Eq. (20) perturbatively order by order. Up to the fourth order of  $\gamma$ , the solution to  $\phi(u)$  can be expressed as

$$\begin{aligned} \frac{\phi(u)}{r_{+c}^z} &= \lambda\phi_1(u) \\ &= \lambda \left( 1 - u^{3-z} + C_7\gamma + C_8\gamma^2 + C_9\gamma^3 + C_{10}\gamma^4 \right), \end{aligned} \tag{21}$$

where  $r_{+c}$  is the location of the horizon at  $T = T_c$ .

Comparing the above solution of  $\phi(u)$  with Eq. (11), we can derive the constant  $\lambda$  as

$$\lambda = \frac{\mu}{r_{+c}^z}. \tag{22}$$

Defining the vector field  $\psi_x(u)$  by a trial function  $F(u)$  as

$$\psi_x(u) = \frac{\langle \hat{J}_x \rangle}{r_{+c}^\Delta} u^\Delta F(u), \tag{23}$$

with the boundary condition  $F(0) = 1$  and  $F'(0) = 0$  [11, 12, 49,51,59,62]. Substituting Eqs. (21) and (23) into Eq. (18)

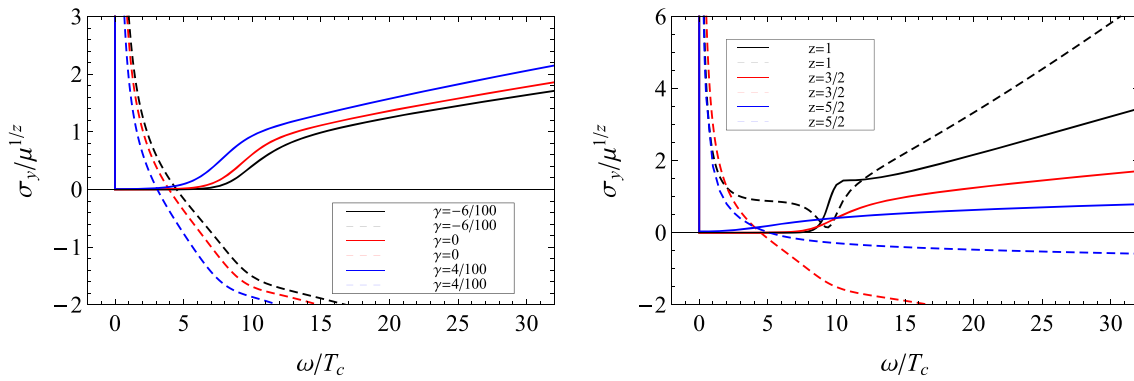


**Fig. 4** The real part (solid) and imaginal part (dashed) of the AC conductivity at  $\frac{T}{T_c} \approx \frac{1}{2}$  as a function of the frequency for fixed  $z = \frac{3}{2}$  with  $\gamma = -\frac{6}{100}$  (black),  $\gamma = 0$  (red),  $\gamma = \frac{4}{100}$  (blue) in the left panel, while the conductivity for fixed  $\gamma = -\frac{6}{100}$  with  $z = 1$  (black),  $z = \frac{3}{2}$  (red) and  $z = \frac{5}{2}$  (blue) in the right panel

yields

$$F''(u) + \frac{z - 2\Delta + (2\Delta + 3)u^{z+3}}{u(u^{z+3} - 1)} F'(u) + \frac{m^2 + \Delta(1 - \Delta + z + (\Delta + 2)u^{z+3})}{u^2(u^{3+z} - 1)} F(u) + \lambda^2 \frac{u^{2z-2} \phi_1(u)^2}{(u^{3+z} - 1)^2} F(u) = 0. \tag{24}$$

According to the condition of  $F(u)$ , we further take the ansatz of  $F(u)$  as

$$F = F_\alpha(u) \equiv 1 - \alpha u^2, \tag{25}$$

with the parameter  $\alpha$  to be determined. Therefore, Eq. (24) can be transformed to the S-L eigenvalue equation

$$(\mathcal{K}F')' - \mathcal{P}F + \lambda^2 \mathcal{Q}F = 0, \tag{26}$$

where the coefficients are respectively

$$\begin{aligned} \mathcal{K} &= \frac{1 - u^{3+z}}{u^{z-2\Delta}}, \\ \mathcal{P} &= \frac{m^2 + \Delta(1 - \Delta + z + (\Delta + 2)u^{3+z})}{u^{2-z-2\Delta}}, \\ \mathcal{Q} &= \frac{u^{2\Delta+z-2} \phi_1(u)^2}{1 - u^{3+z}}. \end{aligned} \tag{27}$$

The eigenvalue of  $\lambda^2$  minimizes the expression with respect to the parameter  $\alpha$  as

$$\lambda^2(z, \gamma, \alpha, u) = \frac{\int_0^1 (\mathcal{K}F'^2 - \mathcal{P}F^2) du}{\int_0^1 \mathcal{Q}F^2 du}. \tag{28}$$

The critical temperature reads

$$T_c = \frac{3 + z}{4\pi\lambda} \mu. \tag{29}$$

We plot the analytical critical temperature as a function of the Weyl parameter  $\gamma$  in the left panel of Fig. 3 in the form of solid point and also list the analytical results in Table 1

for comparison with the numerical results, from which we can see clearly that the analytical results agree well with the numerical ones. In particular, the difference between the analytical and numerical values are within 4% except the case of the boundary of the parameter space ( $z = 1, \gamma = 0.04$  and  $z = \frac{5}{2}, \gamma = -0.06$ ), which indicates that the analytical S-L method is still powerful in the grand canonical ensemble.

Next, we manage to obtain the critical exponent of the vector condensate. Below (but close to) the critical temperature, the vector condensate is very small. Thus we can expand  $\phi(u)$  in the small parameter  $(\langle \hat{J}_x \rangle / r_+^{\Delta+1})^2$  as

$$\frac{\phi(u)}{r_+^z} = \lambda \phi_1(u) + \left( \frac{\langle \hat{J}_x \rangle}{r_+^{\Delta+1}} \right)^2 \chi(u). \tag{30}$$

At the boundary ( $u \rightarrow 0$ ), the function  $\chi(u)$  can be expanded in Taylor series as  $\chi(u) = \chi(0) + \chi'(0)u + \dots$ , and then matching Eq. (30) with Eq. (11), we can obtain

$$\lambda + \chi(0) \left( \frac{\langle \hat{J}_x \rangle}{r_+^{\Delta+1}} \right)^2 = \frac{\mu}{r_+^z}. \tag{31}$$

From Eq. (31), it is clear that the important thing is to derive the value of  $\chi(0)$ . Substituting Eqs. (30) and (23) in Eq. (19) yields the equation of  $\chi(z)$  at the order of  $(\langle \hat{J}_x \rangle)^2$  as

$$\begin{aligned} \chi''(u) + \mathcal{C}_{11} \chi'(u) + \frac{2\lambda F(u)^2 u^{2\Delta} \phi_1(u)}{(u^{z+3} - 1)(6\gamma(z - 5)u^{z+3} + 4\gamma z^2 - 4\gamma z + 1)} &= 0. \end{aligned} \tag{32}$$

Usually, we still take the boundary conditions as  $\chi(1) = 0 = \chi'(1)$  [11, 12, 51, 62]. Multiplying the factor  $u^{z-2}(6\gamma(z - 5)u^{z+3} + 4\gamma z^2 - 4\gamma z + 1)$  to Eq. (32), we can read off

$$\begin{aligned} (u^{z-2}(6\gamma(z - 5)u^{z+3} + 4\gamma z^2 - 4\gamma z + 1)\chi'(u))' &= -2\lambda \frac{F(u)^2 \phi_1(u) u^{2\Delta+z-2}}{u^{z+3} - 1}. \end{aligned} \tag{33}$$

Integrating Eq. (33) with the condition  $\chi'(1) = 0$ , we get

$$\begin{aligned}
 & u^{z-2}(6\gamma(z-5)u^{z+3} + 4\gamma z^2 - 4\gamma z + 1)\chi'(u) \\
 &= 2\lambda \int_{x=u}^{x=1} \frac{F(x)^2 \phi_1(x) x^{2\Delta+z-2}}{x^{z+3} - 1} dx \\
 &= 2\lambda \mathcal{M}(z, \gamma, \alpha, u), \tag{34}
 \end{aligned}$$

where  $\mathcal{M}(z, \gamma, \alpha, u)$  is the function of the Lifshitz parameter  $z$  and the Weyl correction parameter  $\gamma$  as well as the parameter  $\alpha$  and can be given in the explicit form by analytical integration. Integrating further the above equation with  $\chi(1) = 0$ , the value of  $\chi(0)$  reads

$$\begin{aligned}
 \chi(0) &= 2\lambda \int_{u=0}^{u=1} \frac{\mathcal{M}(z, \gamma, \alpha, u)}{u^{z-2}(6\gamma(z-5)u^{z+3} + 4\gamma z^2 - 4\gamma z + 1)} du \\
 &= 2\lambda \mathcal{N}(z, \gamma, \alpha), \tag{35}
 \end{aligned}$$

where  $\mathcal{N}(z, \gamma, \alpha)$  depends on the parameters  $z$  and  $\gamma$  as well as  $\alpha$ . Considering Eqs. (22) and (31) as well as (35), the condensate near the critical temperature can be expressed as

$$\frac{\langle \hat{J}_x \rangle}{r_+^{\Delta+1}} = \frac{1}{\sqrt{-2\mathcal{N}(z, \gamma, \alpha)}} \sqrt{\frac{T_c}{T}} \sqrt{1 - \frac{T}{T_c}}. \tag{36}$$

It is clear that the condensate has a square root behavior near the critical temperature, which agrees with the numerical analysis about the condensate, especially, the grand potential and also indicates a second-order phase transition at the critical point expected from the mean-field theory.

To compare the behavior of condensate for the analytical results with the one of the numerical results in detail, we further process Eq. (36) as

$$\begin{aligned}
 \frac{\langle \hat{J}_x \rangle^{\frac{5}{3}}}{T_c} &= \frac{4\pi}{3+z} \frac{1}{(-2\mathcal{N}(z, \gamma, \alpha))^{\frac{5}{6}}} \left(1 - \frac{T}{T_c}\right)^{\frac{5}{6}} \\
 &= \mathcal{C}(z, \gamma, \alpha) \left(1 - \frac{T}{T_c}\right)^{\frac{5}{6}}, \tag{37}
 \end{aligned}$$

where we have taken into account  $\Delta = 2$  and the approximation  $T \approx T_c$ . After some calculation, we have  $\mathcal{C}(\frac{3}{2}, -\frac{1}{25}, \frac{6571}{10000}) = 7.16813$ ,  $\mathcal{C}(\frac{3}{2}, \frac{1}{25}, \frac{509}{1000}) = 5.55683$ ,  $\mathcal{C}(\frac{5}{2}, -\frac{1}{25}, \frac{5701}{10000}) = 7.70244$ ,  $\mathcal{C}(\frac{5}{2}, \frac{1}{25}, \frac{2239}{5000}) = 9.18543$ . It follows that the vector condensate grows faster with the decreasing Weyl parameter  $\gamma$  for  $z = \frac{3}{2}$  and slower with the decreasing Weyl parameter for  $z = \frac{5}{2}$ , which is again consistent with the behavior of the condensate in Fig. 1.

### 3 Conclusions and discussions

In this paper, we have constructed the holographic  $p$ -wave conductor/superconductor model in the five-dimensional Lifshitz black hole with the Weyl correction via both numerical and analytical methods. We mainly studied the effects of

the dynamical critical exponent  $z$  as well as the Weyl parameter  $\gamma$  on the superconductor model. Main conclusions are as follows.

Firstly, for all values of the Lifshitz parameter  $z$  ( $1 \leq z \leq \frac{5}{2}$ ) and the Weyl parameter  $\gamma$  ( $-\frac{6}{100} \leq \gamma \leq \frac{4}{100}$ ) considered in the present paper, there always exists a critical temperature below which the vector hair starts to condense. The thermodynamical analysis showed that the system undergoes a second-order phase transition at the critical point and the superconducting state is more stable than the normal state below the critical temperature. Meanwhile, at the lower temperature, the difference among the condensate in terms of the fixed Weyl parameters ( $\gamma = -\frac{6}{100}, 0, \frac{4}{100}$ ) decreases with the increasing Lifshitz parameter for  $1 \leq z < 2.35$  and then increases with the increasing Lifshitz parameter  $z$  for  $2.35 < z \leq 2.5$ . This means that the large enough Lifshitz correction can qualitatively alter the effects of the Weyl correction on the condensate. From this perspective, there exists the obvious competition between the Lifshitz correction and the Weyl correction. Furthermore, according to the phase diagram about the critical temperature, when either of two corrections is studied separately, the Lifshitz correction inhibits the phase transition while the Weyl correction enhances the condensate to form. When the two corrections are considered comprehensively, the promoting effects of the Weyl correction are clearly suppressed by the increasing Lifshitz correction, which again reflects the competition of the two corrections to some extent. In addition, the analytical results agree well with the ones from the numerical method, which not only upholds the reliability of the numerical results but also confirms the reasonability of the choice of the present parameter space, especially the Weyl correction parameter  $\gamma$ .

Secondly, for all value of the Lifshitz parameter  $z$ , there is always an obvious pole for the imaginal part of conductivity at the lower frequency, which corresponds to a delta function of the DC conductivity as expected from condensed physics. Meanwhile, at the high frequency, the real part of conductivity increases monotonically, which seems to be the universal behavior for the holographic superconductor model in the five-dimensional gravitational spacetime [34,36,51]. What is more, with the increasing Lifshitz parameter from  $z = 1$ , the minimum of the imaginal part of the conductivity vanishes and the energy gap of the conductivity becomes softer and softer at the intermediate frequency. Furthermore, the real part of conductivity is suppressed with the increasing Lifshitz correction. In addition to the above behavior of the conductivity observed at  $\frac{T}{T_c} \approx 0.5$ , we also calculated the conductivity at or slightly below the critical temperature. It followed that unlike the case for the six order derivative term  $C^2 F^2$  in Refs. [35,63,64], we observed neither the Drude-like peak near the zero-frequency nor the pronounced peak at the intermediate frequency.

It should be noted that even we have read off the reasonable results in the current region of Weyl parameter  $\gamma$  by both numerical and analytical methods, the range of  $\gamma$  is insufficiently rigorous. To obtain the strict range of the Weyl parameter  $\gamma$  in the Lifshitz gravity, it is meaningful to consider the causality violation for the boundary field theory or the superluminal velocity problem in the bulk. Meanwhile, we restricted the present superconductor model in the Lifshitz parameter range  $1 \leq z \leq \frac{5}{2}$ . In principle, so long as  $z < 3$ , we can always read off the regular asymptotical solution from Eq. (11) and thus obtain the critical temperature, the vector condensate as well as the conductivity. However, as we considered the case of  $z = \frac{13}{5}$ , it is difficult to calculate the conductivity at the low frequency for small Weyl correction. In the case of  $z = \frac{14}{5}$ , even the condensate for small Weyl correction takes too long time to read numerically. However, following the phase diagram about the critical temperature, it is expect that we might observe the obvious competing phenomenon between the two corrections at large enough Lifshitz parameter, for example,  $z = \frac{29}{10}$ , i.e., the non-monotonic (or monotonic decreasing) trend of the critical temperature with respect to the Weyl parameter  $\gamma$ . Therefore, it is interesting to extend the parameter space about the Lifshitz parameter for the superconductor model by optimizing the numerical calculation or improving the performance of the equipment. On the other hand, analog to the current coupling between the Weyl tensor and the gauge field, we can also couple the Weyl tensor to the complex vector field, such as the term  $\gamma \rho_{\mu\nu}^\dagger C^{\mu\nu}_{\alpha\beta} \rho^{\alpha\beta}$ . Considering the ansatz of the gauge field and the vector field (7) in the five-dimensional Lifshitz black hole (1), we have found preliminarily that both the Weyl correction  $\gamma$  and the Lifshitz parameter  $z$  are included in the scaling dimension  $\Delta_\pm$  of the vector field, which suggests that the new coupling form will develop much richer effects on the superconductor model. As a result, it is useful and meaningful to investigate the effect of the new coupling correction ( $\gamma \rho_{\mu\nu}^\dagger C^{\mu\nu}_{\alpha\beta} \rho^{\alpha\beta}$ ) on the superconductor models. In the near future, we will try to solve some of the above problems, which will shed light on the understanding of the effect of Weyl correction on our superconductor model in Lifshitz gravity.

**Acknowledgements** We would like to thank Prof. Z. Y. Nie and Q. Y. Pan as well as L. Li for their helpful discussion and comments. This work is supported in part by NSFC (Nos. 11865012, 11647167, 12075109 and 11747615), Foundation of Guizhou Educational Committee (Nos. Qianjiaohe KY Zi [2016]311 Zi), the Foundation of Scientific Innovative Research Team of Education Department of Guizhou Province (201329) and the Fund for Reserve Talents of Young and Middle-aged Academic and Technical Leaders of Yunnan Province (Grant No. 2018HB006).

**Data Availability Statement** This manuscript has no associated data or the data will not be deposited. [Authors' comment: All the calculations were obtained by Mathematica software and not associated with experimental data.]

**Open Access** This article is licensed under a Creative Commons Attribution 4.0 International License, which permits use, sharing, adaptation, distribution and reproduction in any medium or format, as long as you give appropriate credit to the original author(s) and the source, provide a link to the Creative Commons licence, and indicate if changes were made. The images or other third party material in this article are included in the article's Creative Commons licence, unless indicated otherwise in a credit line to the material. If material is not included in the article's Creative Commons licence and your intended use is not permitted by statutory regulation or exceeds the permitted use, you will need to obtain permission directly from the copyright holder. To view a copy of this licence, visit <http://creativecommons.org/licenses/by/4.0/>.  
Funded by SCOAP<sup>3</sup>.

## Appendix: All coefficients denoted by $C_i$ in Sect. 2

In our work, due to the fact that we considered both the high order derivative correction and the Lifshitz spacetime, all the equations of motion (such as the ones for the vector field  $\rho_\mu$ , the perturbative gauge field  $A_y(t, r)$ , especially the solution of the gauge field of  $\phi$ ) are quite long and complicate. In order for the train of thought on the paper to be more clear, we represent the coefficients by the sign  $C_i$ , the concrete forms of which are listed as follows.

$$\begin{aligned}
 C_1 &= 2\gamma r(r f''(r) + (3z - 1)f'(r)) + 4\gamma(z - 1)z f(r) + 1 \\
 C_2 &= 2\gamma r^2 f^{(3)}(r) + 2\gamma r(2z + 5)f''(r) \\
 &\quad - 2\gamma(z^2 - 14z + 5)f'(r) - \frac{4\gamma z(z^2 - 5z + 4)f(r)}{r} \\
 &\quad + \frac{4 - z}{r} \\
 C_3 &= -2\gamma r^2 f''(r) - 2\gamma r(3z - 1)f'(r) - 4\gamma(z - 1)z f(r) + 3 \\
 C_4 &= f'(r) \left( \frac{3}{f(r)} - 2\gamma(7z^2 + 4z - 3) \right) \\
 &\quad - \frac{(z + 2)(4\gamma(z - 1)z f(r) - 3)}{r} - 2\gamma r^2 f^{(3)}(r) \\
 &\quad + \frac{2\gamma r(1 - 3z)f'(r)^2}{f(r)} \\
 &\quad + f''(r) \left( -\frac{2\gamma r^2 f'(r)}{f(r)} - 2\gamma r(4z + 3) \right) \\
 C_5 &= \frac{r^{-2(z+2)}(f(r)(-6\psi(r)^2 r^{2z} - 4\gamma r^2 \omega^2(z - 1)z) + 3r^2 \omega^2)}{f(r)^2} \\
 &\quad - \frac{2\gamma \omega^2 r^{-2z} f''(r)}{f(r)^2} - \frac{2\gamma \omega^2(3z - 1)r^{-2z-1} f'(r)}{f(r)^2} \\
 C_6 &= (6\gamma(z - 5)(2z + 1)u^{z+3} + 4\gamma(z - 2)(z - 1)z + z - 2) \\
 &\quad / u / (6\gamma(z - 5)u^{z+3} + 4\gamma(z - 1)z + 1) \\
 C_7 &= (z^2 - 8z + 15)(-u^{3-z})(u^{z+3} - 1) \\
 C_8 &= (z^2 - 8z + 15)u^{3-z}((5z^3 + 33z^2 - 93z + 135)u^{z+3} \\
 &\quad + 36(z - 5)u^{2z+6} - 5z^3 - 33z^2 + 57z + 45)/(z + 9) \\
 C_9 &= u^{3-z}(z - 3)((5 - z)(z + 6)(z(5z(z(5z + 21) - 150) \\
 &\quad + 1818) - 1035) - 675)u^{z+3} - 36(z - 5)^2(z + 6) \\
 &\quad \times (z(9z - 16) + 15)u^{2z+6} - 108(z - 5)^3(z + 9)u^{3z+9}
 \end{aligned}$$

$$\begin{aligned}
& + (z - 5)(z(z(z(z(5z(5z + 51) + 204) - 2826) + 9) \\
& + 3915) + 4050))/(6 + z)/(9 + z), \\
\mathcal{C}_{10} = & (z - 3)u^{3-z}((z - 5)(z + 5)(z + 9) \\
& \times (z(z(z(z(z(25z(5z + 39) - 2961) - 10881) \\
& + 75897) - 105579) - 15795) + 42525) + 60750)u^{z+3} \\
& + 432(z - 5)^4(z + 6)(z + 9)^2u^{4(z+3)} + 36(z - 5)^2 \\
& \times (z + 5)(z + 6)(z(z(z(z(61z + 329) - 1526) + 2874) \\
& - 1575) - 675)u^{2z+6} + 108(z - 5)^3(z + 5) \\
& \times (z + 9)^2(z(13z - 20) + 15)u^{3z+9} \\
& + (5 - z)(z(z(z(z(z(z(5z(5z(5z + 109) + 3702) \\
& + 17964) - 231930) - 454626) + 1110456) \\
& + 1906092) - 77355) - 4088475) - 3462750)) \\
& / (5 + z)/(6 + z)/(9 + z)^2 \\
\mathcal{C}_{11} = & (12\gamma z^2(u^{z+3} - 1) - 30\gamma u^{z+3} \\
& + z(\gamma(8 - 54u^{z+3}) + 1) + 4\gamma z^3 - 2) \\
& / u / (6\gamma(z - 5)u^{z+3} + 4\gamma z^2 - 4\gamma z + 1)
\end{aligned}$$

## References

- J.M. Maldacena, Adv. Theor. Math. Phys. **2**, 231 (1998). [arXiv:hep-th/9711200](#)
- S.S. Gubser, I.R. Klebanov, A.M. Polyakov, Phys. Lett. B **428**, 105 (1998). [arXiv:hep-th/9802109](#)
- S.A. Hartnoll, A. Lucas, S. Sachdev, [arXiv:1612.07324](#) [hep-th]
- H. Liu, J. Sonner, [arXiv:1810.02367](#) [hep-th]
- R.G. Cai, L. Li, L.F. Li, R.Q. Yang, Sci. China Phys. Mech. Astron. **58**(6), 060401 (2015). [arXiv:1502.00437](#) [hep-th]
- J. Zaanen, Y.W. Sun, Y. Liu, K. Schalm, Cambridge University Press, Cambridge (2015)
- S.A. Hartnoll, C.P. Herzog, G.T. Horowitz, Phys. Rev. Lett. **101**, 031601 (2008). [arXiv:0803.3295](#) [hep-th]
- G.T. Horowitz, M.M. Roberts, Phys. Rev. D **78**, 126008 (2008). [arXiv:0810.1077](#) [hep-th]
- S.A. Hartnoll, C.P. Herzog, G.T. Horowitz, JHEP **0812**, 015 (2008). [arXiv:0810.1563](#) [hep-th]
- K. Maeda, M. Natsuume, T. Okamura, Phys. Rev. D **81**, 026002 (2010). [arXiv:0910.4475](#) [hep-th]
- G. Siopsis, J. Therrien, JHEP **1005**, 013 (2010). [arXiv:1003.4275](#) [hep-th]
- H.-F. Li, JHEP **1307**, 135 (2013). [arXiv:1306.3071](#) [hep-th]
- S.S. Gubser, S.S. Pufu, JHEP **0811**, 033 (2008). [arXiv:0805.2960](#) [hep-th]
- J.-W. Chen, Y.-J. Kao, D. Maity, W.-Y. Wen, C.-P. Yeh, Phys. Rev. D **81**, 106008 (2010). [arXiv:1003.2991](#) [hep-th]
- K.-Y. Kim, M. Taylor, JHEP **1308**, 112 (2013). [arXiv:1304.6729](#) [hep-th]
- Y. Huang, Q. Pan, W.L. Qian, J. Jing, S. Wang, Sci. China Phys. Mech. Astron. **63**(3), 230411 (2020)
- W.C. Yang, C.Y. Xia, H.B. Zeng, H.Q. Zhang, [arXiv:1907.01918](#) [hep-th]
- G.T. Horowitz, B. Way, JHEP **1011**, 011 (2010). [arXiv:1007.3714](#) [hep-th]
- Z.Y. Nie, Q. Pan, H.B. Zeng, H. Zeng, Eur. Phys. J. C **77**(2), 69 (2017). [arXiv:1611.07278](#) [hep-th]
- Z.Y. Nie, H. Zeng, JHEP **1510**, 047 (2015). [arXiv:1505.02289](#) [hep-th]
- E. Kiritsis, L. Li, JHEP **1601**, 147 (2016). [arXiv:1510.00020](#) [cond-mat.str-el]
- R.G. Cai, R.Q. Yang, Phys. Rev. D **91**(2), 026001 (2015). [arXiv:1410.5080](#) [hep-th]
- R.G. Cai, L. Li, Y.Q. Wang, J. Zaanen, Phys. Rev. Lett. **119**(18), 181601 (2017). [arXiv:1706.01470](#) [hep-th]
- S. Cremonini, L. Li, J. Ren, JHEP **1909**, 014 (2019). [arXiv:1906.02753](#) [hep-th]
- Y. Ling, P. Liu, C. Niu, J.P. Wu, Z.Y. Xian, JHEP **1502**, 059 (2015). [arXiv:1410.6761](#) [hep-th]
- R.Q. Yang, H.S. Jeong, C. Niu, K.Y. Kim, JHEP **1904**, 146 (2019). [arXiv:1902.07586](#) [hep-th]
- T. Nishioka, S. Ryu, T. Takayanagi, JHEP **1003**, 131 (2010). [arXiv:0911.0962](#) [hep-th]
- S. Kachru, X. Liu, M. Mulligan, Phys. Rev. D **78**, 106005 (2008). [arXiv:0808.1725](#) [hep-th]
- D.W. Pang, Commun. Theor. Phys. **62**, 265 (2014). [arXiv:0905.2678](#) [hep-th]
- E.J. Brynjolfsson, U.H. Danielsson, L. Thorlacius, T. Zingg, J. Phys. A **43**, 065401 (2010). [arXiv:0908.2611](#) [hep-th]
- Y. Bu, Phys. Rev. D **86**, 046007 (2012). [arXiv:1211.0037](#) [hep-th]
- Z. Fan, JHEP **1309**, 048 (2013). [arXiv:1305.2000](#) [hep-th]
- E. Abdalla, J. de Oliveira, A.B. Pavan, C.E. Pellicer, [arXiv:1307.1460](#) [hep-th]
- J.W. Lu, Y.B. Wu, P. Qian, Y.Y. Zhao, X. Zhang, Nucl. Phys. B **887**, 112 (2014). [arXiv:1311.2699](#) [hep-th]
- J.W. Lu, Y.B. Wu, B.P. Dong, Y. Zhang, Phys. Lett. B **800**, 135079 (2020)
- J.W. Lu, Y.B. Wu, B.P. Dong, H. Liao, Phys. Lett. B **785**, 517 (2018)
- R.G. Cai, S. He, L. Li, L.F. Li, JHEP **1312**, 036 (2013). [arXiv:1309.2098](#) [hep-th]
- R.G. Cai, L. Li, L.F. Li, Y. Wu, JHEP **1401**, 045 (2014). [arXiv:1311.7578](#) [hep-th]
- Y.B. Wu, J.W. Lu, Y.Y. Jin, J.B. Lu, X. Zhang, S.Y. Wu, C. Wang, Int. J. Mod. Phys. A **29**, 1450094 (2014). [arXiv:1405.2499](#) [hep-th]
- Y.B. Wu, J.W. Lu, M.L. Liu, J.B. Lu, C.Y. Zhang, Z.Q. Yang, Phys. Rev. D **89**(10), 106006 (2014). [arXiv:1403.5649](#) [hep-th]
- D. Wen, H. Yu, Q. Pan, K. Lin, W.L. Qian, Nucl. Phys. B **930**, 255 (2018). [arXiv:1803.06942](#) [hep-th]
- Y.B. Wu, J.W. Lu, W.X. Zhang, C.Y. Zhang, J.B. Lu, F. Yu, Phys. Rev. D **90**(12), 126006 (2014). [arXiv:1410.5243](#) [hep-th]
- M. Rogatko, K.I. Wysokinski, JHEP **1603**, 215 (2016). [arXiv:1508.02869](#) [hep-th]
- M. Mohammadi, A. Sheykhi, M. Kord Zangeneh, Eur. Phys. J. C **78**(12), 984 (2018). [arXiv:1901.10540](#) [hep-th]
- R.G. Cai, L. Li, L.F. Li, JHEP **1401**, 032 (2014). [arXiv:1309.4877](#) [hep-th]
- R.G. Cai, L. Li, L.F. Li, R.Q. Yang, JHEP **1404**, 016 (2014). [arXiv:1401.3974](#) [gr-qc]
- Y.B. Wu, J.W. Lu, C.Y. Zhang, N. Zhang, X. Zhang, Z.Q. Yang, S.Y. Wu, Phys. Lett. B **741**, 138 (2015). [arXiv:1412.3689](#) [hep-th]
- A. Sheykhi, H.R. Salahi, A. Montakhab, JHEP **1604**, 058 (2016). [arXiv:1603.00075](#) [gr-qc]
- H.R. Salahi, A. Sheykhi, A. Montakhab, Eur. Phys. J. C **76**(10), 575 (2016). [arXiv:1608.05025](#) [gr-qc]
- R.G. Cai, Z.Y. Nie, H.Q. Zhang, Phys. Rev. D **83**, 066013 (2011). [arXiv:1012.5559](#) [hep-th]
- A. Sheykhi, A. Ghazanfari, A. Dehyadegari, Eur. Phys. J. C **78**(2), 159 (2018). [arXiv:1712.04331](#) [hep-th]
- X.M. Kuang, W.J. Li, Y. Ling, JHEP **1012**, 069 (2010). [arXiv:1008.4066](#) [hep-th]
- R.G. Cai, H.Q. Zhang, Phys. Rev. D **81**, 066003 (2010). [arXiv:0911.4867](#) [hep-th]
- M. Mohammadi, A. Sheykhi, M. Kord Zangeneh, Eur. Phys. J. C **78**(8), 654 (2018). [arXiv:1805.07377](#) [hep-th]

55. B.B. Ghotbabadi, M Kord Zangeneh, A. Sheykhi, Eur. Phys. J. C **78**(5), 381 (2018). [arXiv:1804.05442](#) [hep-th]
56. J. Cheng, Q. Pan, H. Yu, J. Jing, Eur. Phys. J. C **78**(3), 239 (2018). [arXiv:1803.08204](#) [hep-th]
57. A. Ritz, J. Ward, Phys. Rev. D **79**, 066003 (2009). [arXiv:0811.4195](#) [hep-th]
58. J.P. Wu, Y. Cao, X.M. Kuang, W.J. Li, Phys. Lett. B **697**, 153 (2011). [arXiv:1010.1929](#) [hep-th]
59. L. Zhang, Q. Pan, J. Jing, Phys. Lett. B **743**, 104 (2015). [arXiv:1502.05635](#) [hep-th]
60. S .A.Hosseini Mansoori, B. Mirza, A. Mokhtari, F .L. Dezaki, Z. Sherkatghanad, JHEP **1607**, 111 (2016)
61. W. Witzak-Krempa, Phys. Rev. B **89**(16), 161114 (2014). [arXiv:1312.3334](#) [cond-mat.str-el]
62. C. Wang, D. Zhang, G.F.J.P. Wu, W. Jian-Pin, [arXiv:1902.07125](#) [gr-qc]
63. J.P. Wu, P. Liu, Phys. Lett. B **774**, 527 (2017). [arXiv:1710.07971](#) [hep-th]
64. J.W. Lu, Y.B. Wu, B.P. Dong, Y. Zhang, Eur. Phys. J. C **80**(2), 114 (2020)
65. G. Tallarita, Phys. Rev. D **89**(10), 106005 (2014). [arXiv:1402.4691](#) [hep-th]
66. B. Way, Phys. Rev. D **86**, 086007 (2012). [arXiv:1207.4205](#) [hep-th]